tify, especially in patients with a small number of lymph node metastases. Consequently, all the patients in the current study received oral 5-fluorouracil, which is reportedly less toxic than cyclophosphamide, methotrexate, and 5-fluorouracil or doxorubicin and 5-fluorouracil as systemic adjuvant therapy. The local control rate for BCT in Japanese women is also excellent, but the difference is less striking than the survival rate. In our series, the 5-year local control rate for patients with negative, close (≤5 mm), and positive margins was 98.9%, 96.6%, and 92.2%, respectively (27). Local recurrence was usually detected >3 years after BCT in previous studies of MMIBC, and it occurred 10 years after BCT in our study. Therefore, we need longer follow-up and more observation of different ethnicities to reach a firm conclusion. However, our result at this stage suggests that patients with MMIBC can be candidates for BCT, as long as each tumor is operable by breast-conserving surgery criteria and the close surgical margin is accurately detected and treated with adequate boost RT.

REFERENCES

1. Sarrazin D, Le MG, Arriagada R, *et al.* Ten-year results of a randomized trial comparing a conservative treatment to mastectomy in early breast cancer. *Radiother Oncol* 1989;14:177–184.
2. van Dongen JA, Bartelink H, Fentiman IS, *et al.* Randomized clinical trial to assess the value of breast-conserving therapy in stage I and II breast cancer, EORTC 10801 trial. *J Natl Cancer Inst Monogr* 1992;11:15–18.
3. Blichert-Toft M, Rose C, Andersen JA, *et al.*, for the Danish Breast Cancer Cooperative Group. Danish randomized trial comparing breast conservation therapy with mastectomy: Six years of life-table analysis. *J Natl Cancer Inst Monogr* 1992; 11:19–25.
4. Fisher B, Anderson S, Redmond CK, *et al.* Reanalysis and results after 12 years of follow-up in a randomized clinical trial comparing total mastectomy with lumpectomy with or without irradiation in the treatment of breast cancer. *N Engl J Med* 1995;333:1456–1461.
5. Danoff BF, Haller DG, Glick JH, *et al.* Conservative surgery and irradiation in the treatment of early breast cancer. *Ann Intern Med* 1985;102:634–642.
6. Margolese R. Surgical considerations in selecting local therapy. *J Natl Cancer Inst Monogr* 1992;41–48.
7. Veronesi U. NIH consensus meeting on early breast cancer. *Eur J Cancer* 1990;26:843–844.
8. Winchester DP, Cox JD, for the American College of Radiology, American College of Surgeons, College of American Pathologists, Society of Surgical Oncology. Standards for diagnosis and management of invasive breast carcinoma. *CA Cancer J Clin* 1998;48:83–107.
9. Kurtz JM, Jacquemier J, Amalric R, *et al.* Breast-conserving therapy for macroscopically multiple cancers. *Ann Surg* 1990; 212:38–44.
10. Leopold KA, Recht A, Schnitt SJ, *et al.* Results of conservative surgery and radiation therapy for multiple synchronous cancers of one breast. *Int J Radiat Oncol Biol Phys* 1989;16: 11–16.
11. Wilson LD, Beinfield M, McKhann CF, *et al.* Conservative surgery and radiation in the treatment of synchronous ipsilateral breast cancers. *Cancer* 1993;72:137–142.
12. Hartsell WF, Recine DC, Griem KL, *et al.* Should multicentric disease be an absolute contraindication to the use of breast-conserving therapy? *Int J Radiat Oncol Biol Phys* 1994;30: 49–53.
13. Cho LC, Senzer N, Peters GN. Conservative surgery and radiation therapy for macroscopically multiple ipsilateral invasive breast cancers. *Am J Surg* 2002;183:650–654.
14. Kokubo M, Mitsumori M, Yamamoto C, *et al.* Impact of boost irradiation with surgically placed radiopaque clips on local control in breast-conserving therapy. *Breast Cancer* 2001;8: 222–228.
15. Hiraoka M, Mitsumori M, Okajima K, *et al.* Use of a CT simulator in radiotherapy treatment planning for breast conserving therapy. *Radiother Oncol* 1994;33:48–55.
16. Harris JR, Levene MD, Svensson G, Hellman S. Analysis of cosmetic results following primary radiation therapy for stages I and II carcinoma of the breast. *Int J Radiat Oncol Biol Phys* 1979;5:257–261.
17. Andea AA, Wallis T, Newman LA, *et al.* Pathologic analysis of tumor size and lymph node status in multifocal/multicentric breast carcinoma. *Cancer* 2002;94:1383–1390.
18. Fowble B, Yeh IT, Schultz DJ, *et al.* The role of mastectomy in patients with stage I-II breast cancer presenting with gross multifocal or multicentric disease or diffuse microcalcifications. *Int J Radiat Oncol Biol Phys* 1993;27:567–573.
19. DiBiase SJ, Komarnicky LT, Schwartz GF, *et al.* The number of positive margins influences the outcome of women treated with breast preservation for early stage breast carcinoma. *Cancer* 1998;82:2212–2220.
20. Mansfield CM, Komarnicky LT, Schwartz GF, *et al.* Ten-year results in 1070 patients with stages I and II breast cancer treated by conservative surgery and radiation therapy. *Cancer* 1995;75:2328–2336.
21. Wazer DE, Jabro G, Ruthazer R, *et al.* Extent of margin positivity as a predictor for local recurrence after breast conserving irradiation. *Radiat Oncol Invest* 1999;7:111–117.
22. Wazer DE, DiPetrillo T, Schmidt-Ullrich R, *et al.* Factors influencing cosmetic outcome and complication risk after conservative surgery and radiotherapy for early-stage breast carcinoma. *J Clin Oncol* 1992;10:356–363.
23. Bartelink H, Horiot JC, Poortmans P, *et al.* Recurrence rate after treatment of breast cancer with standard radiotherapy with or without additional radiation. *N Engl J Med* 2001;345: 1378–1387.
24. Borger JH, Kemperman H, Smitt HS, *et al.* Dose and volume effects on fibrosis after breast conservation therapy. *Int J Radiat Oncol Biol Phys* 1994;30:1073–1081.
25. Nemoto T, Tominaga T, Chamberlain A, *et al.* Differences in breast cancer between Japan and the United States. *J Natl Cancer Inst* 1977;58:193–197.
26. Yonemoto RH. Breast cancer in Japan and United States: Epidemiology, hormone receptors, pathology, and survival. *Arch Surg* 1980;115:1056–1062.
27. Kokubo M, Mitsumori M, Ishikura S, *et al.* Results of breast-conserving therapy for early stage breast cancer: Kyoto University experiences. *Am J Clin Oncol* 2000;23:499–505.

^{18}F-FDG and ^{11}C-methionine PET for evaluation of treatment response of lung cancer after stereotactic radiotherapy

Takayoshi ISHIMORI, Tsuneo SAGA, Yasushi NAGATA, Yuji NAKAMOTO, Tatsuya HIGASHI, Marcelo MAMEDE, Takahiro MUKAI, Yoshiharu NEGORO, Tetsuya AOKI, Masahiro HIRAOKA and Junji KONISHI

Reprint from Annals of Nuclear Medicine Vol. 18 No. 8
December 2004

Annals of Nuclear Medicine Vol. 18, No. 8, 669–674, 2004

^{18}F-FDG and ^{11}C-methionine PET for evaluation of treatment response of lung cancer after stereotactic radiotherapy

Takayoshi ISHIMORI,* Tsuneo SAGA,* Yasushi NAGATA,** Yuji NAKAMOTO,* Tatsuya HIGASHI,* Marcelo MAMEDE,* Takahiro MUKAI,* Yoshiharu NEGORO,** Tetsuya AOKI,** Masahiro HIRAOKA** and Junji KONISHI*

*Department of Nuclear Medicine and Diagnostic Imaging, Graduate School of Medicine, Kyoto University
**Department of Therapeutic Radiology and Oncology, Graduate School of Medicine, Kyoto University

This study was performed to investigate the feasibility of FDG- and L-[methyl-^{11}C]methionine (Met)-PET for the follow up of lung cancer after stereotactic radiotherapy (SRT). Nine patients (pt) with solitary lung cancer underwent SRT. Met- and FDG-PET studies were performed one week before SRT and from one week to 8 months after SRT. Responses to SRT were complete in 2 pt and partial in 7 pt. Met- and FDG-PET scan showed high tracer uptake in all tumors before SRT. After SRT, standardized uptake values (SUV) of FDG and Met changed concordantly. Both decreased with time in 5 pt but did not decrease steadily in 4 pt, where 2 pt showed an increase at 1 to 2 weeks after SRT and 2 pt showed an increase at more than 3 months after SRT. The former appears to reflect the acute reaction to SRT and the latter radiation-induced pneumonitis. Although the addition of Met-PET did not provide additional information over FDG-PET, FDG- and Met-PET could be used to evaluate the treatment effect of SRT.

Key words: PET, lung cancer, stereotactic radiotherapy, FDG, methionine

INTRODUCTION

POSITRON EMISSION TOMOGRAPHY (PET) with ^{18}F-labeled fluorodeoxyglucose (FDG) has recently been applied widely in clinical oncology.[1–3] However, FDG is not a cancer-specific agent and is known to accumulate in acute inflammation as well as granulomatous and autoimmune diseases.[4–6]

PET with L-[*S*-methyl-^{11}C]methionine (Met) has been used to evaluate the treatment response of lung cancer after conventional irradiation, since Met accumulates less in inflammatory lesions than FDG.[7]

Stereotactic radiotherapy (SRT), which can localize a single high dose selectively to the target, was first applied to the treatment of malignant intracranial tumors, and its feasibility has been reported.[8] Recently, SRT was adopted for lung cancer as an alternative to surgery in patients with solitary lung cancer who did not meet the indications for surgery.[9–11]

The response of a tumor to treatment was conventionally evaluated by measuring the tumor size using morphological imaging modalities such as CT and MRI. However, distinguishing viable residual tumors from fibrotic scars after irradiation is always difficult. Aoki et al. evaluated the CT appearance of tumors and lung injury after SRT, and reported that it was difficult to distinguish residual tumor from radiation fibrosis.[12] For precise differentiation, metabolic imaging such as FDG- and Met-PET may play a major role. Although the feasibility of CT and FDG-PET image fusion in the treatment planning of SRT of lung cancer was reported,[13] there has been no reported study concerning the follow up of lung cancer patients after SRT by PET. The aim of this study was to investigate the feasibility of FDG- and Met-PET for the follow up of lung cancer after SRT.

Received February 25, 2004, revision accepted August 4, 2004.

For reprint contact: Tsuneo Saga, M.D., Department of Nuclear Medicine and Diagnostic Imaging, Graduate School of Medicine, Kyoto University, 54 Kawara-cho, Shogoin, Sakyo-ku, Kyoto 606–8507, JAPAN.

E-mail: saga@kuhp.kyoto-u.ac.jp

PATIENTS AND METHODS

Patients

The study group comprised 9 patients (age range, 64–86 years), who had histologically-confirmed solitary lung cancer less than 4 cm in diameter without distant metastasis and underwent SRT between May, 1999 and February, 2000. The histological diagnoses were: 6 squamous cell carcinomas (SqCC) and 3 adenocarcinomas (Adeno). Details of the individual patients are shown in Table 1. Before being enrolled in this study, each patient gave written informed consent, as required by the Kyoto University Human Study Committee.

Stereotactic Radiotherapy (SRT)

The SRT procedures were previously reported in detail.[11] In brief, radiation therapy was delivered using a 6-MV Linear Accelerator (Clinac 2300C/D Varian Associates, Palo Alto, CA, USA) with the 6 to 10 fields non-coplanar 3D conformal technique. A total tumor isocenter dose of 48 Gy (12 Gy/fraction) was administered in 12 or 13 days. CT (SCT700 TX/TH, Shimadzu Co., Kyoto, Japan) and the three-dimensional treatment planning system (CADPLAN R.6.0.8, Varian Associates, Palo Alto, CA, USA) were used for treatment planning. The Stereotactic Body Frame (Elekta Instrument AB, Stockholm, Sweden) was used for patient fixation.

FDG and Met Preparation

Both FDG and Met were synthesized at the in-house cyclotron facility at Kyoto University Hospital. Fluorine-18 [^{18}F] and carbon-11 [^{11}C] were produced with a cyclotron, CYPRIS-325R (Sumitomo Heavy Industries, Co. Ltd., Tokyo, Japan). ^{18}F-FDG was synthesized by the nucleophilic substitution method with an ^{18}F-FDG-synthesizing instrument, F-100 (Sumitomo Heavy Industries, Co. Ltd., Tokyo, Japan).[14–16]

Met was synthesized by reaction of L-homocysteine thiolactone and [^{11}C]methyl iodide.[16] [^{11}C]Carbon dioxide, produced by a ^{14}N(p, α)^{11}C reaction, was transported into an automated [^{11}C]methyl iodide synthesis system (C-11-BII; Sumitomo Heavy Industries, Co. Ltd., Tokyo, Japan). [^{11}C]Methyl iodide was prepared as previously described,[17] then trapped in a mixture of acetone (500 μl) and 100 mg/ml L-homocysteine thiolactone solution (50 μl). After the addition of 0.2 M NaOH (500 μl), the reaction mixture was heated at 80°C for 3 min. The solution was neutralized with 0.2 M HCl, and evaporated. The resulting residue was then dissolved in sterile saline and passed through a sterile 0.22-μm filter. Radiochemical purity was >97% as determined by analytical HPLC using a Partisil 10-SCX column (4.6×250 mm; Whatman, Clifton, NJ, USA) eluted with 50 mM citric acid/trisodium citrate (10/1).

PET Imaging

One week before SRT, initial Met- and FDG-PET studies were performed on the same day with a dedicated PET scanner (PCT3600W; Hitachi Medical, Tokyo, Japan). This scanner had 8 rings and provided 15 tomographic sections at 7 mm intervals. We certified the scan range, which was marked on the body surface, by referring to CT images previously obtained. All patients fasted for at least 4 hours and underwent a 10-min transmission scan of the lung before Met injection. At the same body position, a Met-PET image was obtained 20 min after intravenous injection of 768.2 ± 224.5 MBq of Met. Sixty min after Met injection, 370.0 ± 37.5 MBq of FDG was intravenously injected and FDG-PET images were obtained 60 min later. At the time of FDG-PET scan, the residual radioactivity of Met was estimated to be 4.6% ± 1.4% of FDG activity. Although Met radioactivity could not be completely eliminated, it was substantially low compared with FDG activity. The emission scan time for both Met- and FDG-PET was 10 min. Attenuation corrected PET images were reconstructed by the filtered back projection method. The tumor uptake of FDG and Met was evaluated semiquantitatively as a standardized uptake value (SUV) in the regions of interest (ROIs) placed over the treated lesion. The ROI placed over the lesion was 10 × 10 mm

Table 1 Patient characteristics

Pt #	Age/Sex	Histology	Local response	Time interval*	Tumor size before SRT**	Tumor size at the maximum response**
1	68/M	SqCC	PR	4 months	3.4×3.3	2.1×2.1
2	74/M	SqCC	PR	2 months	3.2×2.8	2.2×1.8
3	77/F	Adeno.	PR	17 months	2.4×1.7	0.8×0.7
4	77/F	SqCC	CR	3 months	1.7×1.4	0.0×0.0
5	86/M	Adeno.	PR	6 months	2.9×2.7	1.9×1.3
6	70/M	SqCC	CR	11 months	2.1×1.5	0.0×0.0
7	72/M	SqCC	PR	10 months	3.4×1.7	1.0×0.8
8	71/M	SqCC	PR	16 months	3.3×3.1	1.0×1.0
9	71/M	Adeno.	PR	16 months	3.1×2.5	2.6×0.6

*: time interval between SRT and maximum response on CT

**: long axis × short axis (cm) on CT images

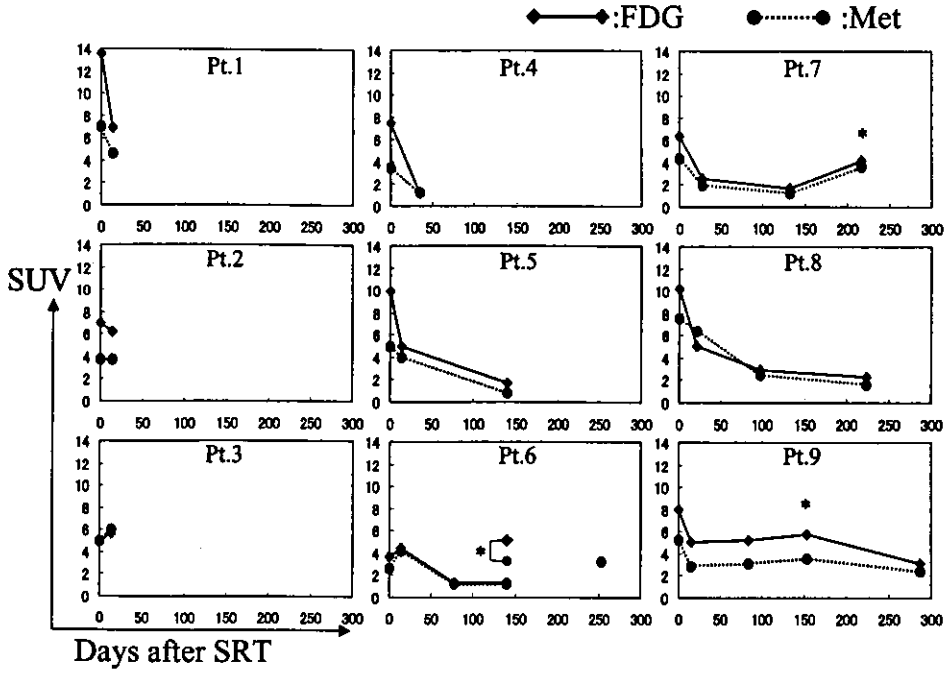

Fig. 1 The temporal changes in SUV in 9 patients are shown. (◆—◆ FDG, ●---● Met) In pt. 6, increased uptake of FDG and Met are observed (*) corresponding to the SRT-induced pneumonitis separated from the treated tumor. In pt. 7 and pt. 9, increased uptakes (*) are observed because the treated tumors are involved in SRT-induced pneumonitis.

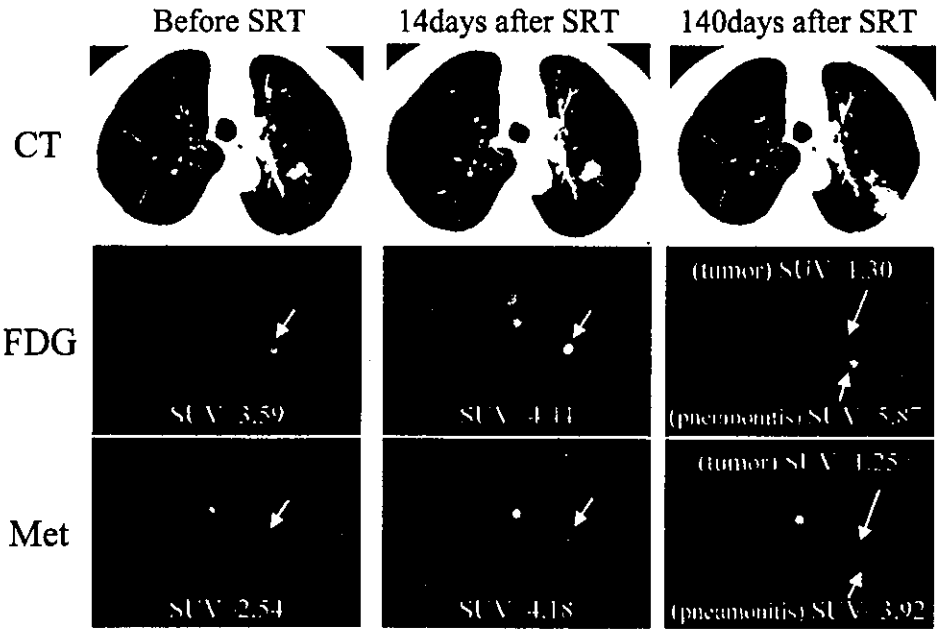

Fig. 2 (patient #6). (*Left*) Before treatment, CT shows a mass lesion (1.5 cm) in the left lower lung (S6). FDG- and Met-PET show high tracer uptake in the tumor. (*Middle*) Fourteen days after SRT, both FDG- and Met-PET show higher uptake in the tumor than in the pre-treatment study. The corresponding CT shows slight enlargement of the treated tumor. (*Right*) One hundred and forty days after SRT, the uptake of FDG and Met to the tumor is decreased, while both FDG- and Met-PET show higher uptake in the peripheral lung field. CT shows a decrease in tumor size. Furthermore, CT reveals a new consolidation in the peripheral lung field suggestive of radiation-induced pneumonitis, corresponding to the high uptake of FDG and Met. One year later, follow-up CT showed a decrease in size of this opacity (not shown).

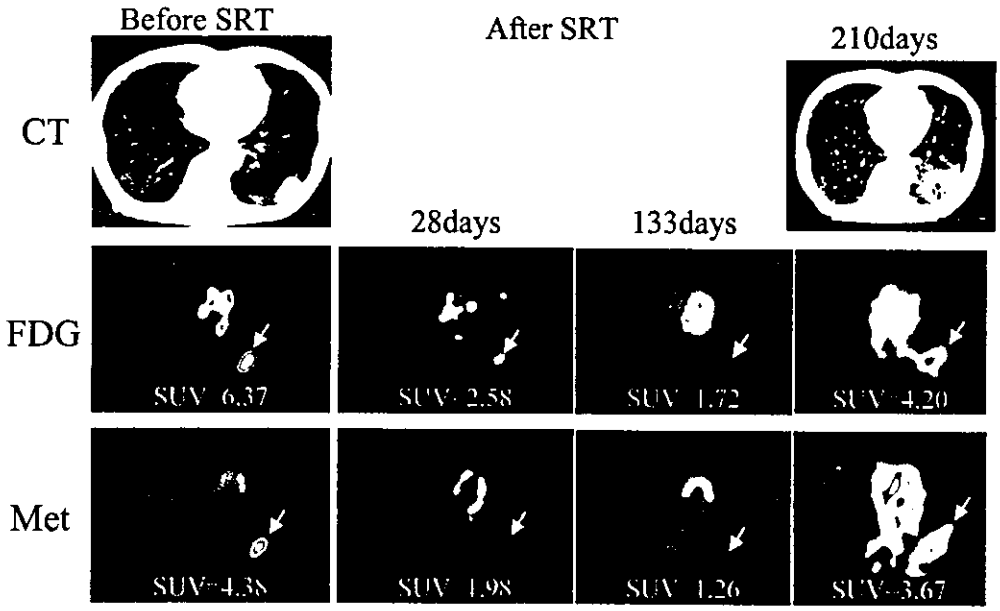

Fig. 3 (patient #7). (*Left*) Before treatment, CT shows a mass (3 cm) in the left lower lung (S9). FDG- and Met-PET show high tracer uptake in the tumor. (*Middle*) Both at 28 and 133 days after SRT, the uptakes of FDG and Met in the tumor have decreased steadily. (*Right*) Seven months after SRT, CT shows consolidation surrounding the tumor area, consistent with radiation-induced pneumonitis. FDG- and Met-PET show higher uptake in the corresponding area. The uptake of the tumor cannot be separated from that of inflammation.

(independent of tumor size) and was placed in tumor areas that showed the highest tracer activity. The SUV was calculated as the mean value in this ROI. Follow-up PET studies were performed in the same manner from 2 weeks to 8 months after SRT. Overall, 56 (28 Met- and 28 FDG-) PET examinations were conducted for these 9 patients.

The tumor size was also evaluated by CT images before and after SRT, and a local response was defined according to the Response Evaluation Criteria in Solid Tumors (RECIST) as follows[18]:

CR (complete response): no visible tumor

PR (partial response): 30% or greater decrease in tumor diameter

NC (no change): less than 30% reduction or less than 20% increase in tumor diameter

PD (progressive disease): 20% or greater increase in tumor diameter

The local response was evaluated at the time of maximum local response, and the time interval between SRT and evaluation of response was from 2 months to 17 months (Table 1).

RESULTS

The temporal changes in SUV of FDG and Met are shown in Figure 1. The local response of the treated tumor evaluated by CT images was complete response (CR) in 2 patients and partial response (PR) in 7 patients. An initial PET study showed high FDG and Met uptake to the tumors in all patients. In the follow up studies, SUV of FDG and Met had decreased gradually with time in 5 patients. In contrast, in the remaining 4 patients, SUV of FDG and Met did not decrease steadily, with 2 patients (Pt. 3 and 6) showing a temporal increase in SUV of both FDG and Met at 2 weeks after SRT, and 2 patients (Pt. 7 and 9) showing a delayed increase of both SUVs more than 3 months after SRT (Figs. 2 and 3). In the latter two patients, CT showed the presence of radiation-induced pneumonitis in the treated area. An additional patient (Pt. 6) developed radiation pneumonitis in the vicinity of the tumor site about 5 months later, which showed increased FDG uptake, although the FDG-uptake in the treated tumor remained low. In all cases, changes in the tumor uptake of Met paralleled those of FDG, and there was no discrepancy between Met and FDG uptake changes.

DISCUSSION

SRT is a new and attractive technique, which can localize a high radiation dose selectively to the target. It is reported clinically effective and can be performed safely without serious complications.[10] However, the temporal changes in tumor viability or metabolism after this treatment have not been clarified. The response of tumor tissue to SRT might be different from that to conventional radiotherapy since the single dose is higher and the overall treatment time is shorter in SRT.

In the follow up of lung cancer patients, tumor size measurements using CT have been the standard method of the evaluation of the treatment response,[18] but it could be falsely positive after treatment due to the fibrotic or necrotic tissue remaining in the tumor. Differentiating residual tumor from radiation fibrosis is also difficult in lung cancer patients after SRT.[12]

FDG-PET, which can depict tumor glucose metabolism, is widely used for the evaluation of malignant tumors in clinical oncology. Since FDG is a good marker of tumor viability, FDG-PET is also widely applied for the evaluation of lung cancer after treatment.[19,20] However, Haberkorn et al. reported the contribution of inflammatory reactions caused by radiation injury in falsely increased FDG uptake after radiation therapy.[21] FDG has some limitations in the evaluation of an irradiated tumor because it is known to accumulate not only in malignant cells but also in inflammatory reactions. Met is an essential amino acid necessary for protein synthesis. The transport and metabolism of Met are increased in malignant cells,[7] and Met-PET is useful in the evaluation of lung cancer.[22] Met uptake in tumor tissue is reported to be more specific for viable cancer cells than FDG, where granulation tissue and macrophages show lower uptake of Met.[7] Therefore, Met-PET appears to be more suitable for the monitoring of the treatment response of cancers.[23]

In the present study, all patients showed a favorable response to SRT (2 CRs & 7 PRs) with no treatment failures noted. In 5 of 9 patients, tumor uptake of both tracers (FDG & Met) decreased with time, implying the feasibility of FDG- and Met-PET in the follow up of patients after SRT. However, in the remaining 4 patients, tumor uptake of both tracers did not decrease steadily. In 2 patients, a temporal increase in SUVs of both tracers at 1 to 2 weeks after SRT appeared to reflect the acute reaction of the tumor to SRT.[24] In the other 2 patients, the delayed increase in both SUVs at more than 3 months after SRT occurred along with the appearance of radiation-induced pneumonitis at the site of the tumor. In an additional patient, pneumonitis at the vicinity of the tumor showed increased FDG and Met uptake, while FDG and Met uptakes in the treated tumor were low. In these 3 patients, therefore, it is highly likely that both FDG and Met accumulated in the inflammatory tissue of radiation-induced pneumonitis.

The present results, namely the accumulation of Met in the inflammatory change evoked by SRT, were not consistent with our initial expectations of a difference between the two tracers. Only a few studies have described Met uptake in inflammatory[25] or granulomatous[26] lesions, and the exact reason why Met accumulated in SRT-induced inflammation is not clear. Higashi et al. reported from an *in vitro* study that the increased FDG and Met uptake in cancer cells observed 12 days after irradiation could be attributed to giant-cell formation and accelerated repair of cells.[27] They suggested that tumor cells themselves could transiently increase FDG and Met uptake early after irradiation. Among the present 5 patients who had a temporal increase in the uptake of FDG and Met in the tumor, this mechanism may have occurred in 2 cases in which increased tracer uptake was observed 1 to 2 weeks after SRT. However, in the 3 other patients, in whom an increase of both tracer uptakes occurred at more than 3 months after SRT, an acute reaction of cancer cells was not the likely cause and the increased uptake could only be explained by the contribution of infiltrating inflammatory cells in SRT-induced pneumonitis, which actively accumulated both tracers. In the follow up of patients after SRT, Met-PET did not provide any additional information to that obtained from FDG-PET and was not useful in distinguishing an inflammatory reaction evoked by SRT.

To evaluate the precise treatment effect by FDG- and/or Met-PET, the contribution of inflammatory reactions after SRT, which includes both the acute reaction and irradiation-induced pneumonitis, should be minimized. Aoki et al. reported that the initial changes of the irradiated lung detected by CT appeared 2–6 months after SRT.[12] In this small number of cases, no temporal increases of FDG or Met uptake were observed between 2 weeks and 2 months after SRT. FDG- and Met-PET might possibly evaluate the treatment effect without interference from inflammation during this period. However, the number of patients was quite small, and further studies are warranted to optimize the timing of the PET examination after SRT of lung cancer.

In the present study, it was not fully evaluated whether FDG- and Met-PET provided additional information over CT scan. Although PET imaging is expected to have additional value over morphological imaging such as CT or MR, further studies are needed to elucidate the impact of PET images as compared to morphological imaging modalities.

CONCLUSIONS

The present study showed, for the first time, that FDG- and Met-PET could be used for the follow up of lung cancer patients after SRT, although the addition of Met-PET did not provide additional information to that gained from FDG-PET. Further investigations are necessary to elucidate the optimal timing of FDG- and Met-PET examinations after SRT to evaluate the precise treatment effect.

REFERENCES

1. Delbeke D. Oncological applications of FDG PET imaging: brain tumors, colorectal cancer, lymphoma and melanoma. *J Nucl Med* 1999; 40: 591–603.
2. Strauss LG. Positron Emission Tomography: Current Role for Diagnosis and Therapy Monitoring in Oncology.

Oncologist 1997; 2: 381–388.
3. Inokuma T, Tamaki N, Torizuka T, Fujita T, Magata Y, Yonekura Y, et al. Value of fluorine-18-fluorodeoxyglucose and thallium-201 in the detection of pancreatic cancer. *J Nucl Med* 1995; 36: 229–235.
4. Shreve PD. Focal fluorine-18 fluorodeoxyglucose accumulation in inflammatory pancreatic disease. *Eur J Nucl Med* 1998; 25: 259–264.
5. Strauss LG. Fluorine-18 deoxyglucose and false-positive results: a major problem in the diagnostics of oncological patients. *Eur J Nucl Med* 1996; 23: 1409–1415.
6. Nakamoto Y, Saga T, Ishimori T, Higashi T, Mamede M, Okazaki K, et al. FDG-PET of autoimmune-related pancreatitis: preliminary results. *Eur J Nucl Med* 2000; 27: 1835–1838.
7. Kubota R, Kubota K, Yamada S, Tada M, Takahashi T, Iwata R, et al. Methionine uptake by tumor tissue: a microautoradiographic comparison with FDG. *J Nucl Med* 1995; 36: 484–492.
8. Auchter RM, Lamond JP, Alexander E, Buatti JM, Chappell R, Friedman WA, et al. A multiinstitutional outcome and prognostic factor analysis of radiosurgery for resectable single brain metastasis. *Int J Radiat Oncol Biol Phys* 1996; 35: 27–35.
9. Uematsu M, Shioda A, Suda A, Fukui T, Ozeki Y, Hama Y, et al. Computed tomography-guided frameless stereotactic radiotherapy for stage I non-small cell lung cancer: a 5-year experience. *Int J Radiat Oncol Biol Phys* 2001; 51: 666–670.
10. Nagata Y, Negoro Y, Aoki T, Mizowaki T, Takayama K, Kokubo M, et al. Clinical outcomes of 3D conformal hypofractionated single high-dose radiotherapy for one or two lung tumors using a stereotactic body frame. *Int J Radiat Oncol Biol Phys* 2002; 52: 1041–1046.
11. Negoro Y, Nagata Y, Aoki T, Mizowaki T, Araki N, Takayama K, et al. The effectiveness of an immobilization device in conformal radiotherapy for lung tumor: reduction of respiratory tumor movement and evaluation of the daily setup accuracy. *Int J Radiat Oncol Biol Phys* 2001; 50: 889–898.
12. Aoki T, Nagata Y, Negoro Y, Takayama K, Mizowaki T, Kokubo M, et al. Evaluation of lung injury after three-dimensional conformal stereotactic radiation therapy for solitary lung tumors: CT appearance. *Radiology* 2004; 230: 101–108.
13. Giraud P, Grahek D, Montravers F, Carette MF, Deniaud-Alexandre E, Julia F, et al. CT and (18)F-deoxyglucose (FDG) image fusion for optimization of conformal radiotherapy of lung cancers. *Int J Radiat Oncol Biol Phys* 2001; 49: 1249–1257.
14. Kitano H, Magata Y, Tanaka A, Mukai T, Kuge Y, Nagatsu K, et al. Performance assessment of O-18 water purifier. *Ann Nucl Med* 2001; 15: 75–78.
15. Hamacher K, Coenen HH, Stocklin G. Efficient stereospecific synthesis of no-carrier-added 2-[^{18}F]-fluoro-2-deoxy-D-glucose using aminopolyether supported nucleophilic substitution. *J Nucl Med* 1986; 27: 235–238.
16. Comar D, Cartron J, Maziere M, Marazano C. Labelling and metabolism of methionine-methyl-^{11}C. *Eur J Nucl Med* 1976; 1: 11–14.
17. Magata Y, Saji H, Tokui T, Ohmomo Y, Yamada Y, Hirata M, et al. High reactivity of [^{11}C]CH_3I with thiol group in the synthesis of C-11 labeled radiopharmaceuticals. *Ann Nucl Med* 1993; 7: 173–177.
18. Therasse P, Arbuck SG, Eisenhauer EA, Wanders J, Kaplan RS, Rubinstein L, et al. New guidelines to evaluate the response to treatment in solid tumors. European Organization for Research and Treatment of Cancer, National Cancer Institute of the United States, National Cancer Institute of Canada. *J Natl Cancer Inst* 2000; 92: 205–216.
19. Kubota K. From tumor biology to clinical PET: A review of positron emission tomography (PET) in oncology. *Ann Nucl Med* 2001; 15: 471–486.
20. Abe Y, Matsuzawa T, Fujiwara T, Itoh M, Fukuda H, Yamaguchi K, et al. Clinical assessment of therapeutic effects on cancer using ^{18}F-2-fluoro-2-deoxy-D-glucose and positron emission tomography: preliminary study of lung cancer. *Int J Radiat Oncol Biol Phys* 1990; 19: 1005–1010.
21. Haberkorn U, Strauss LG, Dimitrakopoulou A, Engenhart R, Oberdorfer F, Ostertag H, et al. PET studies of fluorodeoxyglucose metabolism in patients with recurrent colorectal tumors receiving radiotherapy. *J Nucl Med* 1991; 32: 1485–1490.
22. Kubota K, Matsuzawa T, Fujiwara T, Ito M, Hatazawa J, Ishiwata K, et al. Differential diagnosis of lung tumor with positron emission tomography: a prospective study. *J Nucl Med* 1990; 31: 1927–1932.
23. Kubota K, Yamada S, Ishiwata K, Ito M, Fujiwara T, Fukuda H, et al. Evaluation of the treatment response of lung cancer with positron emission tomography and L-[methyl-^{11}C]methionine: a preliminary study. *Eur J Nucl Med* 1993; 20: 495–501.
24. Plowman PN. Stereotactic radiosurgery. VIII. The classification of postradiation reactions. *Br J Neurosurg* 1999; 13: 256–264.
25. Ishii K, Ogawa T, Hatazawa J, Kanno I, Inugami A, Fujita H, et al. High L-methyl-[^{11}C]methionine uptake in brain abscess: a PET study. *J Comput Assist Tomogr* 1993; 17: 660–661.
26. Yamada Y, Uchida Y, Tatsumi K, Yamaguchi T, Kimura H, Kitahara H, et al. Fluorine-18-fluorodeoxyglucose and carbon-11-methionine evaluation of lymphadenopathy in sarcoidosis. *J Nucl Med* 1998; 39: 1160–1166.
27. Higashi K, Clavo AC, Wahl RL. *In vitro* assessment of 2-fluoro-2-deoxy-D-glucose, L-methionine and thymidine as agents to monitor the early response of a human adenocarcinoma cell line to radiotherapy. *J Nucl Med* 1993; 34: 773–779.

Radiology

Tetsuya Aoki, MD
Yasushi Nagata, MD, PhD
Yoshiharu Negoro, MD, PhD
Kenji Takayama, MD
Takashi Mizowaki, MD, PhD
Masaki Kokubo, MD, PhD
Natsuo Oya, MD, PhD
Michihide Mitsumori, MD, PhD
Masahiro Hiraoka, MD, PhD

Index terms:
Lung neoplasms, CT, 60.12112
Lung neoplasms, therapeutic radiology, 60.32, 60.33
Radiations, injurious effects, complications of therapeutic radiology
Stereotaxis
Therapeutic radiology, three-dimensional

Published online before print
10.1148/radiol.2301021226
Radiology 2004; 230:101–108

Abbreviations:
SRT = stereotactic radiation therapy
V20 = percentage volume of the whole lung irradiated by more than 20 Gy in total

[1] From the Department of Therapeutic Radiology and Oncology, Graduate School of Medicine, Kyoto University, 54 Shogoin Kawahara-cho, Sakyo, Kyoto 606-8507, Japan. Received September 25, 2002; revision requested December 10; final revision received May 17, 2003; accepted June 18. Supported by grants-in-aid no. 09255255, no. 10153231, and no. 13470183 from the Ministry of Education, Culture, Sports, Science, and Technology, and no. 23765293 from the Ministry of Health, Labour, and Welfare in Japan. **Address correspondence to** Y. Nagata (e-mail: *nag@kuhp.kyoto-u.ac.jp*).

Author contributions:
Guarantor of integrity of entire study, Y. Nagata; study concepts, T.A.; study design, Y. Nagata; literature research, T.A.; clinical studies, all authors; data acquisition, T.A.; data analysis/interpretation, T.A., Y. Nagata; statistical analysis, T.A.; manuscript preparation, T.A., Y. Nagata; manuscript definition of intellectual content and editing, Y. Nagata; manuscript revision/review and final version approval, T.A., Y. Nagata, M.H.

Evaluation of Lung Injury after Three-dimensional Conformal Stereotactic Radiation Therapy for Solitary Lung Tumors: CT Appearance[1]

PURPOSE: To evaluate the computed tomographic (CT) appearance of tumors and lung injury in patients who have undergone stereotactic radiation therapy (SRT) for solitary lung tumors.

MATERIALS AND METHODS: Twenty-seven patients with primary lung cancer and four with metastatic lung cancer who underwent SRT for solitary lung tumors were enrolled for evaluation. SRT was delivered by using a three-dimensional conformal technique with a stereotactic body frame. A total dose of 48 Gy was administered in four fractions during a period of 2 weeks. After SRT, follow-up CT images were obtained every 2–3 months. Radiation-induced pulmonary injuries were classified into four patterns on CT images. The minimal lung dose to areas demonstrating pulmonary injury at CT was evaluated, and the correlation between the dose and the percentage volume of the whole lung irradiated by more than 20 Gy in total (V20) was assessed by using Spearman rank correlation.

RESULTS: Tumor shrinkage continued for 2–15 months after SRT. Asymptomatic changes in the irradiated lung were noted at CT in all patients within 2–6 months (median, 4 months) after SRT. As the pattern at pulmonary CT changed, patchy consolidation was more predominantly seen as an acute change than were slight homogeneous increase in opacity, discrete consolidation, or solid consolidation; solid consolidation was the more predominantly seen late change. The minimal lung dose to the area demonstrating pulmonary injury in each patient ranged between 16 and 36 Gy (median, 24 Gy). The dose was significantly ($P < .001$) inversely correlated with the V20 in each patient.

CONCLUSION: The reaction to SRT of the lungs seems similar to the reaction to conventional radiation therapy.

The techniques of three-dimensional conformal radiation therapy and patient immobilization have recently been developed, which enables us to focus high doses of irradiation on the target area and relatively less irradiation on normal tissues. In radiation therapy for solitary lung tumors, the local control may be improved safely by using these techniques to deliver a higher dose to only the target volume. The results of several clinical studies on hypofractionated high-dose stereotactic radiation therapy (SRT) with the three-dimensional conformal radiation therapy technique for irradiation of solitary lung tumors have been reported (1–7).

It was considered that the clinical and radiographic appearances of radiation-induced pulmonary change caused by hypofractionated SRT would not be similar to the change induced by conventional radiation therapy because of differences in the total radiation

dose, dose per fraction, dose distribution, overall treatment time, and other variables (2–8). Few reports have demonstrated computed tomographic (CT) images associated with hypofractionated SRT of lung tumors, although the CT findings after conventional radiation therapy have been reported previously (9–14). Thus, the purpose of our study was to evaluate the CT appearance of tumors and lung injury in patients who have undergone SRT of solitary lung tumors.

TABLE 1
Histologic Diagnoses of Primary Lung Cancer Types

Diagnosis	No. of Patients (n = 27)
Adenocarcinoma	15 (56)
Squamous cell carcinoma	9 (33)
Small cell carcinoma	1 (4)
Unknown	2 (7)

Note.—Data in parentheses are percentages.

TABLE 2
Primary Lesions of Metastatic Lung Tumors

Primary Lesion	No. of Patients (n = 4)
Colon cancer	1
Oral floor cancer	1
Osteosarcoma	1
Tongue cancer	1

TABLE 3
Response Evaluation Criteria in Solid Tumors

Response	Definition
Complete response	The complete disappearance of the tumor for more than 4 weeks
Partial response	At least 30% decrease in the maximal diameter of the target
Stable disease	Between 30% decrease and 20% increase in the maximal diameter of the target
Progressive disease	At least 20% increase in the maximal diameter of the target

MATERIALS AND METHODS

Patients

Since July 1998, three-dimensional conformal SRT with a body frame has been performed in patients with solitary lung tumors at our institution with the approval of our institutional review board and with written informed consent from all patients (4,8). The study reported here comprised 40 patients who were treated with this technique between July 1998 and November 2000.

The eligibility criteria for patients with primary lung cancer were as follows: *(a)* a solitary pulmonary nodule without nodal or distant metastases (T1–3N0M0) was present, *(b)* tumor size was less than 40 mm in diameter, *(c)* the patient could remain stable in the body frame for more than 30 minutes, *(d)* oxygen was not normally required, *(e)* the histologic findings could be confirmed, *(f)* surgery was contraindicated or refused, and *(g)* the spinal cord could be kept out of the high-dose area (5 Gy per fraction). The eligibility criteria for patients with metastatic lung cancer were as follows: *(a)* one or two pulmonary nodules were present, *(b)* tumor size was less than 40 mm in diameter, *(c)* the patient could remain stable in the body frame for more than 30 minutes, *(d)* oxygen was not normally required, *(e)* the spinal cord could be kept out of the high-dose area (5 Gy per fraction), and *(f)* the primary tumor was controlled.

Of the 40 patients, 34 (27 with primary lung cancer and seven with metastatic lung tumor) were irradiated with 48 Gy in total, three were irradiated with 40 Gy in total, and three were irradiated with 60 Gy in total. In this study, of the 34 patients irradiated with 48 Gy, 31 patients (27 with primary lung cancer and four with metastatic lung tumor) treated for single tumors were enrolled for analysis; three patients with metastatic tumors, who were treated for two tumors each, were excluded. Among the 27 patients with primary lung cancer, the histologic diagnosis was confirmed with transbronchial lung biopsy or percutaneous biopsy results in 25 patients. The histologic diagnoses are shown in Table 1. The clinical stages of primary lung cancer were T1N0M0 in 16 patients, T2N0M0 in eight patients, and T3N0M0 in three patients. The primary lesions in the four patients with metastatic lung tumors are shown in Table 2. The pulmonary function and clinical background (presence of chronic obstructive pulmonary disease, quantity of cigarettes smoked, and other factors) of the patients were not closely evaluated in this study.

Treatment with SRT

A stereotactic body frame (Elekta Instruments, Stockholm, Sweden) was used to fix the patient's body. The details of patient fixation and treatment planning were described in our previous reports (4,8). CT images were obtained with a CT simulator (CT Target; Shimadzu, Kyoto, Japan). CT scanning was performed with a 1- or 3-mm section thickness and interval. Cadplan (Varian Associates, Palo Alto, Calif) was used as the three-dimensional treatment-planning system. Radiation therapy was delivered by using a 6-MV linear accelerator (Clinac 2300C/D, Varian Associates) with a three-dimensional noncoplanar conformal technique using five to 10 fields. The planning target volume was set with a margin of 5–10 mm to the clinical target volume that was directly delineated with the three-dimensional treatment-planning system. The total radiation dose at the isocenter was 48 Gy administered over a period of 2 weeks, and the daily fraction size was 12 Gy. Dose-volume relationships for the planning target volume and organs at risk, such as the lung and spinal cord, were calculated by the treatment-planning system. The target dose homogeneity was planned to be within 15%, and the percentage volume of the whole lung irradiated by more than 20 Gy in total (V20) was planned to be less than 10%.

CT Imaging

Follow-up CT examinations (Xvigor; Toshiba Medical Systems, Tokyo, Japan) were performed regularly every 2–3 months in the 1st year after radiation therapy and every 3–6 months thereafter for the evaluation of tumor response and the detection of radiation-induced pulmonary injury after SRT. CT examinations were performed by using a conventional nonhelical technique at 120 kVp, 200 mAs, 5-mm collimation around the tumor, and 10-mm collimation at other sites. One hundred milliliters of nonionic iodinated contrast agent were administered intravenously at a rate of 1.0 mL/sec (for the initial 40.0 mL) and 0.5 mL/sec (for the remainder) by using an automatic injector, and the scanning delay was 60 seconds.

The tumor response at CT was evaluated by using both lung window (level, −700 HU; width, 900 HU) and soft-tissue

TABLE 4
National Cancer Institute's Common Toxicity Criteria in the Lung

Adverse Event	Grade 0	1	2	3	4
Cough	Absent	Mild, relieved by nonprescription medication	Requiring narcotic antitussive	Severe cough or coughing spasms, poorly controlled or unresponsive to treatment	...
Dyspnea	Normal	...	Dyspnea on exertion	Dyspnea at normal level of activity	Dyspnea at rest or requiring ventilator support
Pneumonitis/ pulmonary infiltrates	None	Radiographic changes but asymptomatic or symptoms not requiring steroids	Radiographic changes and requiring steroids or diuretics	Radiographic changes and requiring oxygen	Radiographic changes and requiring assisted ventilation
Pulmonary fibrosis	None	Radiographic changes but asymptomatic or symptoms not requiring steroids	Requiring steroids or diuretics	Requiring oxygen	Requiring assisted ventilation

TABLE 5
Maximal Response on CT Images

Response	No. of Patients (n = 31)
Complete response	5 (16)
Partial response	24 (77)
Stable disease	0 (0)
Progressive disease	2 (6)

Note.—Data in parentheses are percentages.

window (level, 60 HU; width, 400 HU) settings. Response Evaluation Criteria in Solid Tumors, or RECIST, was used for the evaluation of therapeutic efficacy on CT images (15) (Table 3). The tumor sizes were measured by a board-certified radiologist (T.A.) by using a CT image obtained at the isocenter level. If the tumor location changed because of a change in lung volume at follow-up CT, the tumor size was measured on the section in which the tumor appeared to show the largest size. The National Cancer Institute's Common Toxicity Criteria (16) (Table 4) were used to evaluate clinical complications of the respiratory tract. Grading was performed by one of the authors (Y. Nagata). The CT appearance of radiation-induced pulmonary injury was classified into four patterns (by T.A.) according to the categories reported by Libshitz and Shuman (10): *(a)* homogeneous slight increase in opacity that uniformly involves the irradiated portions, *(b)* patchy consolidation within the irradiated lung that does not conform to the shape of radiation portal, *(c)* discrete consolidation that conforms to the shape of the radiation portal but does not uniformly outline it, and *(d)* solid consolidation that conforms to and totally involves the irradiated portions of the lung.

In SRT, the direction of radiation portals is more complicated than it is in conventional radiation therapy; therefore, it was difficult to accurately compare the shape of the radiation portals with the shape of pulmonary change. For that reason, in this study, the patterns of radiation-induced pulmonary change were evaluated by extending the Libshitz and Shuman definitions by considering the dose distribution at treatment-planning CT. If the pulmonary injury contained more than one of the classification patterns, the dominant one was recorded. In addition to this classification, we tried to classify the CT findings of pulmonary change according to the shape and extent of change. The shape of pulmonary change was classified into three patterns: *(a)* wedge shape, *(b)* round shape, and *(c)* irregular shape. The extent of pulmonary change was classified into four patterns: *(a)* peripheral extent, *(b)* central extent, *(c)* a mixed pattern of peripheral and central extent, and *(d)* a skip lesion, which was isolated from the tumor.

In areas that demonstrated radiation-induced pulmonary injury at CT, the threshold lung dose was evaluated by one of the authors (T.A.), who compared the dose distribution at the treatment-planning CT examination and the maximal extent of pulmonary changes at the follow-up CT examination. The isodose curve was made for every 4 Gy in total at treatment-planning CT, and an image fusion between the treatment-planning CT images and the follow-up CT images was manually established by referring to the bony structures. Since the extent of pulmonary injury did not always conform to the isodose curve, the minimal dose in the area demonstrating the pulmonary changes was recorded. If the volume of the involved lung changed, surrounding structures on the CT images, such as pulmonary vessels, bronchi, or fissures, were also used for reference. In addition, the correlation between the minimal lung dose and V20 was evaluated to assess whether there was a dose-volume relationship affecting the likelihood of pulmonary injury.

Statistical Analysis

Spearman rank correlation coefficient was used to assess the correlation between the minimal lung dose (when radiation-induced pulmonary injury appeared on CT images) and V20. Statistical significance was defined by $P < .05$.

RESULTS

The planning target volume was 0.5–38.6 cm^3 (median, 15.1 cm^3). The maximum dose of the planning target volume was 100.4%–105.0% (median, 102.3%), and the minimum dose of the planning target volume was 84.7%–96.9% (median, 92.5%) of the isocenter dose. The V20 was 1.0%–11.6% (median, 4.6%).

Patients underwent follow-up CT examinations for 2–31 months (median, 14 months) after SRT. The maximal responses on CT images were complete response in five patients, partial response in 24 patients, and progressive disease in two patients (Table 5). Thus, the overall response rate (combined complete response and partial response) was 94% (29 of 31). In some cases it was difficult to distinguish the residual tumor from radiation fibrosis, and, therefore, we assessed

any suspicious residual irregular density after SRT as a residual tumor.

The tumor response or shrinkage continued for 2–15 months (median, 6 months) after radiation therapy. The changes in tumor size in all 31 patients after SRT are presented in Figure 1. Two (6%) of 31 patients had no tumor regression and had continuous progression. These two patients had metastatic lung tumors. Therefore, within the time frame of this study, only two patients with metastatic lung tumors developed local recurrence, while none of the patients with primary lung cancer developed local recurrence. Four patients with primary lung cancer and two with metastatic lung tumors died during the follow-up period. Autopsy was not performed in any of these patients.

Changes in the normal lung at CT were noted in all 31 patients. However, none developed severe (grade 2 or higher, Table 4) symptomatic pulmonary complications. All 31 patients developed grade 1 pneumonitis, and the performance status was not worsened in any patient after SRT. The changes in the lung at CT developed 2–6 months (median, 4 months) after SRT, and chronic radiation fibrosis with volume loss appeared 6–15 months (median, 11 months) after SRT. The CT findings of radiation-induced pulmonary change are summarized in Table 6, and CT images showing representative examples of the clinical course after radiation therapy are shown in Figures 2–8. As an acute change, a patchy consolidation pattern was predominantly seen (Figs 2, 3), followed by a homogeneous, slight increase in opacity (Fig 4). As a late change, a solid consolidation pattern was predominantly seen (Figs 2, 5), followed by a discrete consolidation (Fig 6). In regard to the shape and spread of the pulmonary change, a wedge (Fig 7) or round (Fig 8) shape and peripheral spread from the tumor were mainly seen.

In comparison with the dose distribution of treatment-planning CT examinations and the extent of radiation-induced pulmonary change at the follow-up CT examinations, the minimal lung dose for which pulmonary injury appeared at CT for each patient ranged between 16 and 36 Gy (median, 24 Gy). An example of the correlation between dose distribution and radiation-induced pulmonary change at CT is shown in Figure 9. The minimal dose of pulmonary change was significantly ($P < .001$) inversely correlated with the V20 (Fig 10).

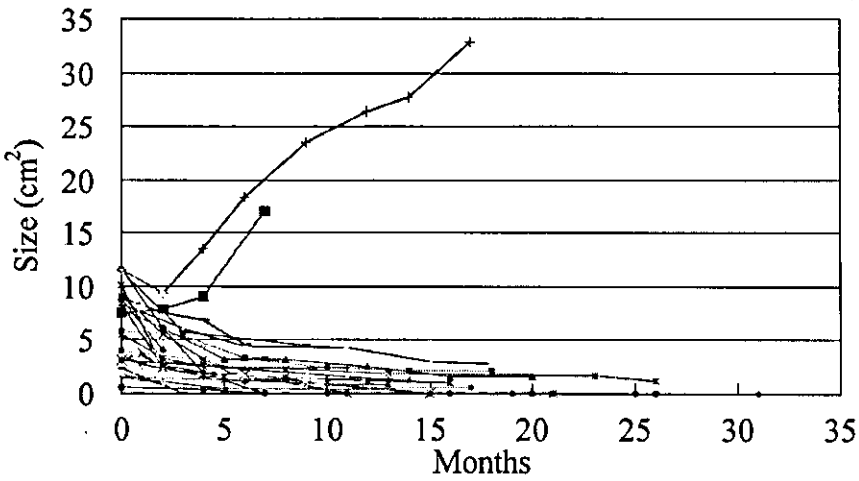

Figure 1. Graph shows the changes in tumor sizes in all patients. The tumor size was measured as the product of the widest diameter and the perpendicular diameter of the target. Measurements were obtained in the CT image showing the greatest tumor size of each image set.

TABLE 6
Summary of CT Findings of Radiation Pneumonitis

Finding	No. of Patients
Pattern*	
≤6 months after SRT (n = 31)	
No change	0 (0)
Homogeneous, slight increase in opacity	8 (26)
Patchy consolidation	21 (68)
Discrete consolidation	2 (6)
Solid consolidation	0 (0)
>6 months after SRT (n = 26)	
No change	0 (0)
Homogeneous, slight increase in opacity	0 (0)
Patchy consolidation	2 (8)
Discrete consolidation	7 (27)
Solid consolidation	17 (65)
Shape (n = 31)	
Wedge	11 (35)
Round	11 (35)
Irregular	9 (29)
Extent (n = 31)	
Peripheral	15 (48)
Mixed peripheral/central	12 (39)
Central	2 (6)
Skip lesion	2 (6)

Note.—Data in parentheses are percentages.
* If pneumonitis showed more than one of the classification patterns, the dominant pattern was recorded.

DISCUSSION

In our study, the complete response and partial response rates in all patients were 16% (five of 31) and 77% (24 of 31), respectively, and the overall (combined complete and partial) response rate was as high as 94%, although our median follow-up period was short (14 months). However, the actual complete response rate may have been higher than shown because it was difficult to accurately distinguish a tumor from radiation-induced pulmonary change in some cases, and we assessed any suspicious masslike shadow after SRT to be a tumor.

It was sometimes difficult to distinguish radiation-induced pulmonary change from a tumor, presumably because of the difference in the shape of the irradiated lung between SRT and conventional radiation therapy. In SRT, multiple noncoplanar portals with various directions were used. The shape of the dose distribution with a

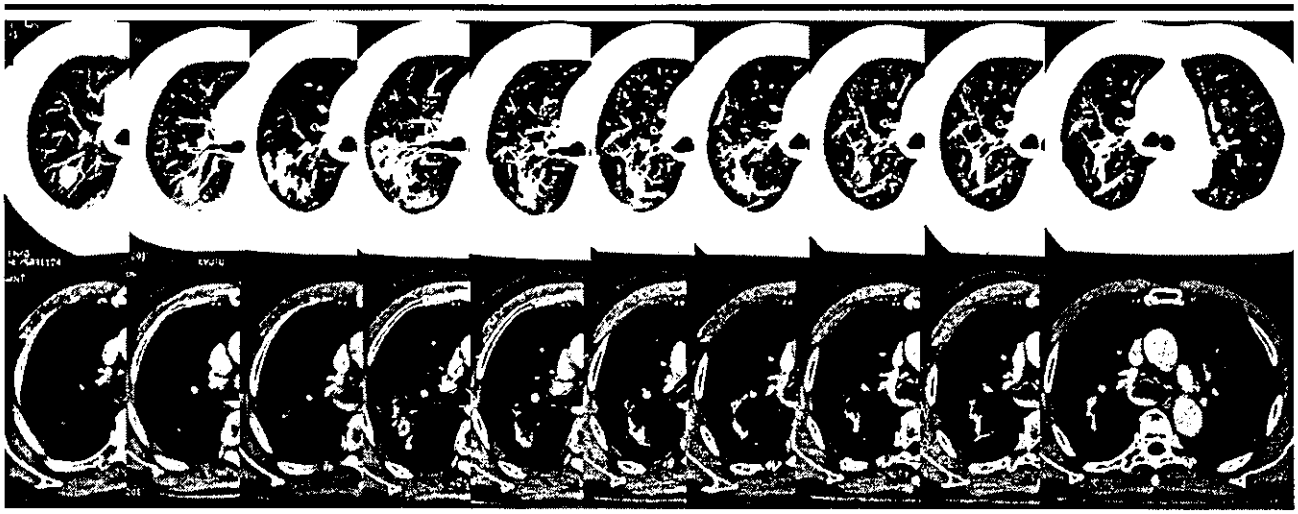

Figure 2. Transverse CT images obtained in a 69-year-old man with primary lung cancer (T1N0M0, adenocarcinoma) show a representative case of the clinical course after SRT. The irregularly shaped patchy consolidation and homogeneous slight increase in opacity appeared around the tumor 4 months after SRT; after 6 months, a new patchy consolidation appeared. Afterward, the patchy consolidation diminished and changed to solid consolidation with scarring. Although it can not be accurately distinguished between the residual tumor and the solid consolidation in the image 15 months after SRT, no recurrence was observed, even in the 25- and 31-month images, and the tumor was considered as showing partial response.

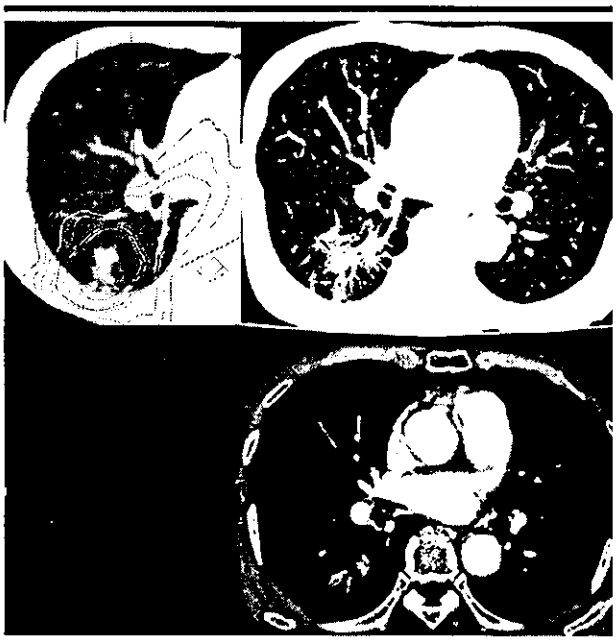

Figure 3. Transverse CT images show a representative case of patchy consolidation. Left: Image obtained for treatment planning at the isocenter. Right and bottom: Images obtained 5 months after SRT show an irregularly shaped consolidation that does not conform to the dose distribution curve. It is visible with the lung window setting (top right) and can be partially detected with the soft-tissue window setting (bottom).

Figure 4. Transverse CT images show a representative case of homogeneous slight increase in opacity. Left: Image obtained for treatment planning at the isocenter. Right and bottom: Images obtained 6 months after SRT. The opacity around the tumor (arrow) was slightly and homogeneously increased with the lung window setting (top right), and there were no abnormal shadows around the tumor with the soft-tissue window setting (bottom).

lower dose tended to become large and irregular, while a higher dose could be concentrated uniformly on the tumor. In contrast, in conventional radiation therapy, the shape of the dose distribution of irradiated lungs was simple, and the boundary between the nonirradiated and irradiated lung was usually distinct. In the evaluation of the patients who have undergone SRT, radiologists should not hastily judge volume progression around the tumor to be local recurrence. Of course, it is an essential

Figure 5. Transverse CT images show a representative case of solid consolidation. Left: Image obtained for treatment planning at the isocenter. Right and bottom: Images obtained 13 months after SRT. Consolidation involving the tumor and surrounding lung tissue in the treatment-planning CT image was observed with the lung window setting (top right), and most of this consolidation was detectable with the soft-tissue window setting (bottom).

Figure 6. Transverse CT images show a representative case of discrete consolidation. Left: Image obtained for treatment planning at the isocenter. Right and bottom: Images obtained 10 months after SRT. Consolidation (arrows) involving the high-dose area (≥ 24 Gy) (not strictly conforming to the 24 Gy isodose line) in the treatment-planning CT image was observed with the lung window setting (top right) and could be partially detected with the soft-tissue window setting (bottom).

problem to determine whether viable cells are present in the fibrotic scar after SRT. In this study, autopsies were not performed in any patients. Therefore, we could not confirm the results by using histologic examination, and, at present, close follow-up studies are necessary to make a correct diagnosis. Other modalities, such as positron emission tomography, may also help in evaluating the tumor response and detecting tumor recurrence (17–19).

In this study, tumor shrinkage lasted 2–15 months (median, 6 months) after SRT; that is, even if a higher radiation dose was delivered with hypofractionated SRT in comparison with the radiation dose with conventional radiation therapy, the tumor did not always reduce rapidly.

The CT appearances of pulmonary changes after conventional radiation therapy were classified by Libshitz and Shuman (10) into four patterns, as stated previously. The homogeneous pattern and the patchy pattern correspond to the acute exudative phase of radiation-induced injury, the discrete pattern corresponds to the organizing or proliferative phase, and the solid pattern corresponds to the chronic fibrotic phase (14). In our study, this classification was extended to SRT because the shape of the dose distribution differed from that in conventional radiation therapy. As a result, the patterns could be grouped by using the Libshitz and Shuman classification. In our study, the patchy consolidation pattern was predominantly seen as an acute change, and the solid consolidation pattern, which would reflect radiation fibrosis, was predominantly seen as a late change.

In conventional radiation therapy, acute pulmonary changes usually occur about 1–8 months after the completion of radiation therapy (10,12,14,20,21). In this study, the initial pulmonary changes at CT appeared 2–6 months after the completion of radiation therapy, which is similar to the results in conventional radiation therapy. If a new pulmonary opacity coinciding with the high-dose area (≥16 Gy) appears within 6 months after SRT, radiologists should consider the appearance of radiation-induced pulmonary change.

Chronic fibrous changes were also evaluated in our study. The solid consolidation pattern, which was regarded as chronic fibrous change, was seen 6–15 months after SRT, and no solid consolidation was seen as the predominant pattern until more than 6 months after SRT in this study. The solid consolidation pattern was usually observed 6–24 months after conventional radiation therapy (12,14,20).

It is important to note that none of the patients with pulmonary changes on transverse CT images had clinically severe (grade 2 or more) symptoms in this study. The reason is assumed to be that the lung volume irradiated with a very high dose was relatively small, and there was sufficient nonirradiated lung tissue since the lung is regarded as the parallel organ. Graham et al (22,23) reported the correlation between radiation pneumonitis and the dose-volume relationship in three-dimensional conformal radiation therapy with conventional fractionation. In the study by Graham et al (22), the

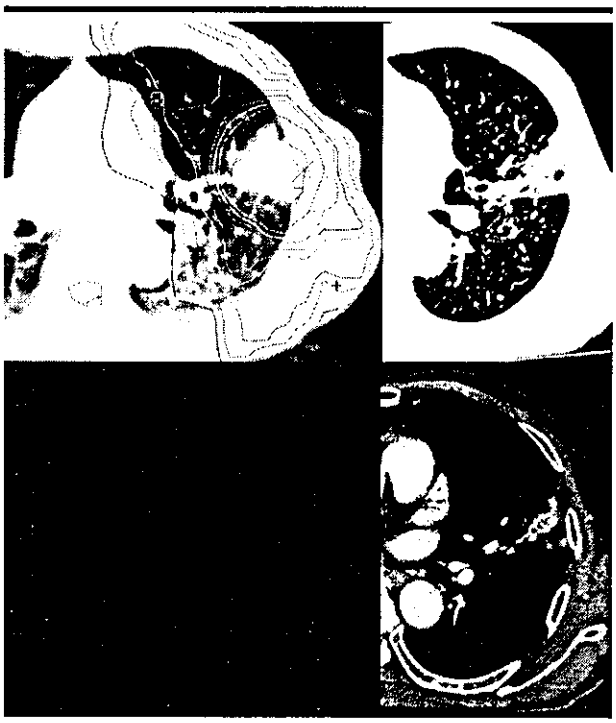

Figure 7. Transverse CT images show a representative case of wedge-shaped radiation-induced pulmonary injury. Left: Image obtained for treatment planning at the isocenter. Right and bottom: Images obtained 5 months after SRT. Wedge-shaped discrete consolidation involving the hilar and peripheral side of the tumor was observed. This shadow did not conform to any isodose curves.

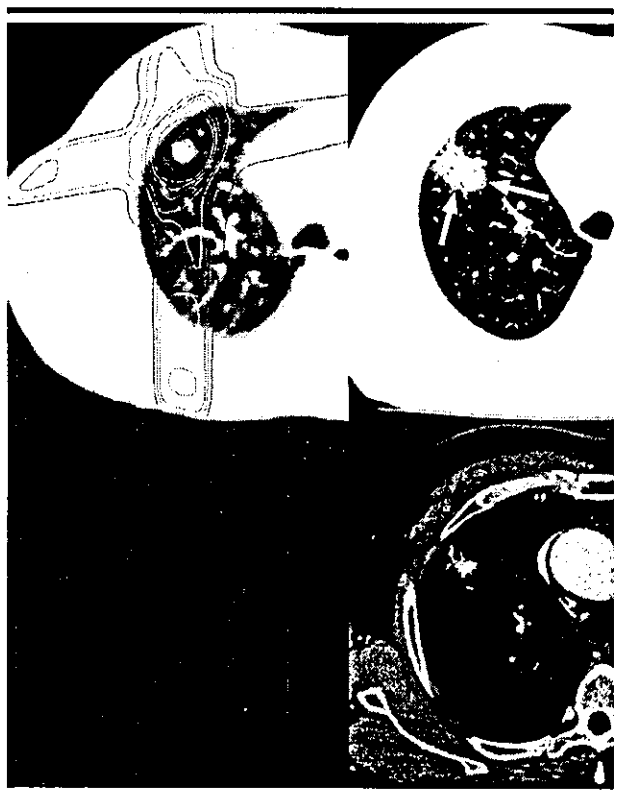

Figure 8. Transverse CT images show a representative case of round-shaped radiation-induced pulmonary injury. Left: Image obtained for treatment planning at the isocenter. Right and bottom: Images obtained 4 months after SRT. Round-shaped patchy consolidation was observed around the tumor (arrows).

Figure 9. CT image shows the isodose curve superimposed on radiation-induced pulmonary change 4 months after SRT. In this case, the pulmonary change (contoured with a thick dashed line) appeared on and within the 16-Gy line (thick solid line). The outer thin dashed line indicates the 12-Gy line, and the inner thin solid line indicates the 20-Gy line.

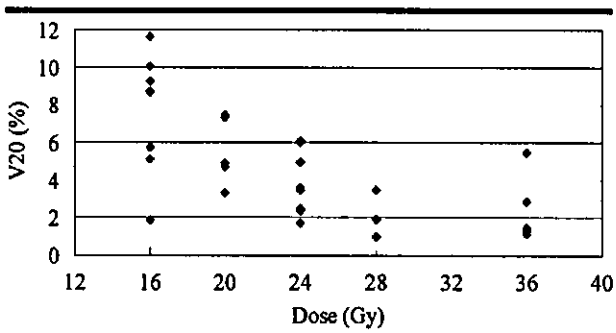

Figure 10. Graph shows correlation between the minimal dose at which radiation-induced pulmonary change occurred and the V20. The dose distribution at CT generated by the three-dimensional treatment-planning system and the radiation-induced pulmonary changes at follow-up CT were compared, and the minimal dose for the appearance of pulmonary change was determined. There was a significant inverse correlation between the minimal dose and V20.

V20 was significantly ($P = .001$) correlated with the presence of grade 2 or higher radiation pneumonitis, and if the V20 was less than 25%, 25%–37%, or more than 37%, the incidence of radiation pneumonitis would be estimated at 0%–4%, 2%–12%, or 19%–30%, respectively. In our study, the V20 in all patients was less than 25%; therefore, it is consistent that none of our patients developed clinically important pneumonitis from the point of the dose-volume

relationship. However, further investigation will be needed as to whether applying the results of Graham et al directly to our own is appropriate, because the fraction size and overall treatment time were different between conventional radiation therapy and SRT.

In our study, the pulmonary function and clinical background of the patients were not closely evaluated. Therefore, further evaluation that includes the change in pulmonary function is desirable.

In this study, the minimal dose for which pulmonary injury appeared on CT images of each patient was 16–36 Gy. These doses were substantially lower in patients with a higher V20. That is, the minimal dose to the injured lung was related to the percentage volume that received more than 20 Gy. Although a dose-volume relationship has been reported for the occurrence of radiation injury in the rectum after prostate cancer treatment (24,25), to our knowledge ours is a new finding not previously reported for lung injury. The cells for repair may migrate in the injured lung from the normal tissue that received a low dose, and the further that low-dose region is from the region of injury, the less likely it is that the injured cell can be repaired. This explanation is only speculative, and our follow-up period was not very long. Therefore, further follow-up studies are necessary.

In conclusion, the CT appearance of radiation-induced pulmonary injury from SRT of the lung seems similar to that from conventional radiation therapy. However, the extension of the change on CT images should be interpreted by considering the shape of dose distribution peculiar to SRT.

Acknowledgment: The authors gratefully acknowledge Daniel Mrozek, BS, for helping with the English translation.

References

1. Blomgren H, Lax I, Naslund I, Svanstrom R. Stereotactic high dose fraction radiation therapy of extracranial tumors using an accelerator: clinical experience of the first thirty-one patients. Acta Oncol 1995; 34:861–870.
2. Wulf J, Hadinger U, Oppitz U, Thiele W, Ness-Dourdoumas R, Flentje M. Stereotactic radiotherapy of targets in the lung and liver. Strahlenther Onkol 2001; 177:645–655.
3. Takai Y, Mituya M, Nemoto K, et al. Simple method of stereotactic radiotherapy without stereotactic body frame for extracranial tumors. Nippon Igaku Hoshasen Gakkai Zasshi 2001; 61:403–407.
4. Nagata Y, Negoro Y, Aoki T, et al. Clinical outcomes of 3D conformal hypofractionated single high-dose radiotherapy for one or two lung tumors using a stereotactic body frame. Int J Radiat Oncol Biol Phys 2002; 52:1041–1046.
5. Nakagawa K, Aoki Y, Tago M, Terahara A, Ohtomo K. Megavoltage CT-assisted stereotactic radiosurgery for thoracic tumors: original research in the treatment of thoracic neoplasms. Int J Radiat Oncol Biol Phys 2000; 48:449–457.
6. Uematsu M, Shioda A, Suda A, et al. Computed tomography-guided frameless stereotactic radiotherapy for stage I non-small cell lung cancer: a 5-year experience. Int J Radiat Oncol Biol Phys 2001; 51:666–670.
7. Uematsu M, Shioda A, Tahara K, et al. Focal, high dose, and fractionated modified stereotactic radiation therapy for lung carcinoma patients: a preliminary experience. Cancer 1998; 82:1062–1070.
8. Negoro Y, Nagata Y, Aoki T, et al. The effectiveness of an immobilization device in conformal radiotherapy for lung tumor: reduction of respiratory tumor movement and evaluation of the daily setup accuracy. Int J Radiat Oncol Biol Phys 2001; 50:889–898.
9. Ikezoe J, Takashima S, Morimoto S, et al. CT appearance of acute radiation-induced injury in the lung. AJR Am J Roentgenol 1988; 150:765–770.
10. Libshitz HI, Shuman LS. Radiation-induced pulmonary change: CT findings. J Comput Assist Tomogr 1984; 8:15–19.
11. Mah K, Poon PY, Van Dyk J, Keane T, Majesky IF, Rideout DF. Assessment of acute radiation-induced pulmonary changes using computed tomography. J Comput Assist Tomogr 1986; 10:736–743.
12. Mesurolle B, Qanadli SD, Merad M, et al. Unusual radiologic findings in the thorax after radiation therapy. RadioGraphics 2000; 20:67–81.
13. Pagani JJ, Libshitz HI. CT manifestations of radiation-induced change in chest tissue. J Comput Assist Tomogr 1982; 6:243–248.
14. Park KJ, Chung JY, Chun MS, Suh JH. Radiation-induced lung disease and the impact of radiation methods on imaging features. RadioGraphics 2000; 20:83–98.
15. Therasse P, Arbuck SG, Eisenhauer EA, et al. New guidelines to evaluate the response to treatment in solid tumors: European Organization for Research and Treatment of Cancer, National Cancer Institute of the United States, National Cancer Institute of Canada. J Natl Cancer Inst 2000; 92:205–216.
16. Trotti A, Byhardt R, Stetz J, et al. Common toxicity criteria: version 2.0 an improved reference for grading the acute effects of cancer treatment—impact on radiotherapy. Int J Radiat Oncol Biol Phys 2000; 47:13–47.
17. Inoue T, Kim EE, Komaki R, et al. Detecting recurrent or residual lung cancer with FDG-PET. J Nucl Med 1995; 36:788–793.
18. Patz EF Jr, Lowe VJ, Hoffman JM, Paine SS, Harris LK, Goodman PC. Persistent or recurrent bronchogenic carcinoma: detection with PET and 2-[F-18]-2-deoxy-D-glucose. Radiology 1994; 191:379–382.
19. Kubota K. From tumor biology to clinical PET: a review of positron emission tomography (PET) in oncology. Ann Nucl Med 2001; 15:471–486.
20. Seppenwoolde Y, Lebesque JV. Partial irradiation of the lung. Semin Radiat Oncol 2001; 11:247–258.
21. Libshitz HI, DuBrow RA, Loyer EM, Charnsangavej C. Radiation change in normal organs: an overview of body imaging. Eur Radiol 1996; 6:786–795.
22. Graham MV, Purdy JA, Emami B, et al. Clinical dose-volume histogram analysis for pneumonitis after 3D treatment for non-small cell lung cancer (NSCLC). Int J Radiat Oncol Biol Phys 1999; 45:323–329.
23. Graham MV. Predicting radiation response. Int J Radiat Oncol Biol Phys 1997; 39:561–562.
24. Skwarchuk MW, Jackson A, Zelefsky MJ, et al. Late rectal toxicity after conformal radiotherapy of prostate cancer (I): multivariate analysis and dose-response. Int J Radiat Oncol Biol Phys 2000; 47:103–113.
25. Jackson A, Skwarchuk MW, Zelefsky MJ, et al. Late rectal bleeding after conformal radiotherapy of prostate cancer. II. Volume effects and dose-volume histograms. Int J Radiat Oncol Biol Phys 2001; 49: 685–698.

原 著

論文受付
2003年3月5日

論文受理
2003年9月24日

Code Nos. 431
524
534

放射線治療におけるポータルイメージの自動照合プログラムの開発

赤澤博之・中森伸行[1)]・塩本敦子[2)]・矢野慎輔[2)]・岡田 孝[2)]
小川憲一[2)]・小松龍一[2)]・森本美穂[2)]・高倉 亨[2)]
永田 靖[3)]・平岡眞寛[3)]

京都大学医学部附属病院放射線部
(現 京都医療技術短期大学診療放射線技術学科)
1)京都工芸繊維大学工芸学部電子情報工学科
2)京都大学医学部附属病院放射線部
3)京都大学大学院医学研究科放射線医学講座腫瘍放射線科学

緒 言

放射線治療の目的は，病巣周囲の正常組織に対する障害を可能な限り少なくし，臨床標的体積に対して計画した線量を正確に，かつ高い位置精度で照射することである．しかしながら，高エネルギーX線を用いた外部照射では，位置決めから実際の照射にいたる過程で，さまざまな機械的誤差と人為的誤差が入り込む．これらの誤差を減らし，高い位置精度で外部照射を行うためには，正確な照射野照合が必要である[1)]．照射野照合の方法としては，従来からX線フィルムを用いた写真照合が主流であり，最近ではelectronic portal imaging devices(EPID)も臨床で使用されるようになってきた．しかし，どちらの場合でも目視による照射野照合のため，観察者の主観や経験などで差が生じたり，ときには誤りが起こった．

わが国でも過去に，照合写真による照射位置の再現性に関する報告[2~4)]があるが，臨床では目視による評価が主流であり，客観的な照射野照合の手法についての報告はない．

本研究では，シミュレーションイメージとポータル

Development of Automatic Verification System for Portal Image in Radiotherapy

HIROYUKI AKAZAWA, NOBUYUKI NAKAMORI,[1)] ATSUKO SHIOMOTO,[2)] SHINSUKE YANO,[2)] TAKASHI OKADA,[2)] KENICHI OGAWA,[2)] RYUUICHI KOMATSU,[2)] MIHO MORIMOTO,[2)] TOORU TAKAKURA,[2)] YASUSHI NAGATA,[3)] and MASAHIRO HIRAOKA[3)]

Clinical Radiology Service, Kyoto University Hospital
(Present address: Department of Radiological Technology, Kyoto College of Medical Technology)
1)Department of Electronics and Information Science, Kyoto Institute of Technology
2)Clinical Radiology Service, Kyoto University Hospital
3)Department of Therapeutic Radiology and Oncology, Kyoto University, Graduate School of Medicine

Received March 5, 2003; Revision accepted Sept. 24, 2003; Code Nos. 431, 524, 534

Summary

The current method of verification for external beam radiation therapy visually compares a simulation image with a portal image. However, because this method depends largely upon the observer's experience, it sometimes results in inter-observer differences. In this study, we developed software to measure atomatically the quantitative difference between the simulation image and portal image using an image-analysis method. The feasibility of this software was evaluated on a rectangular field in the pelvic region. We took 12 simulation images of a pelvic phantom, setting 4 different field shapes on each of 3 isocenters. We then obtained 84 portal images setting 7 known distances from each of the 12 simulation images. Using this software, the direction of shift was detected correctly, and the distance of shift was detected correctly to within less than 3 mm. We consider that this software could be a useful method of verification.

Key words: Automated verification, Simulation image, Portal image, Pelvic region, Image processing

別刷資料請求先：〒622-0041 京都府船井郡園部町小山東町今北1-3
京都医療技術短期大学 診療放射線技術学科 赤澤博之 宛

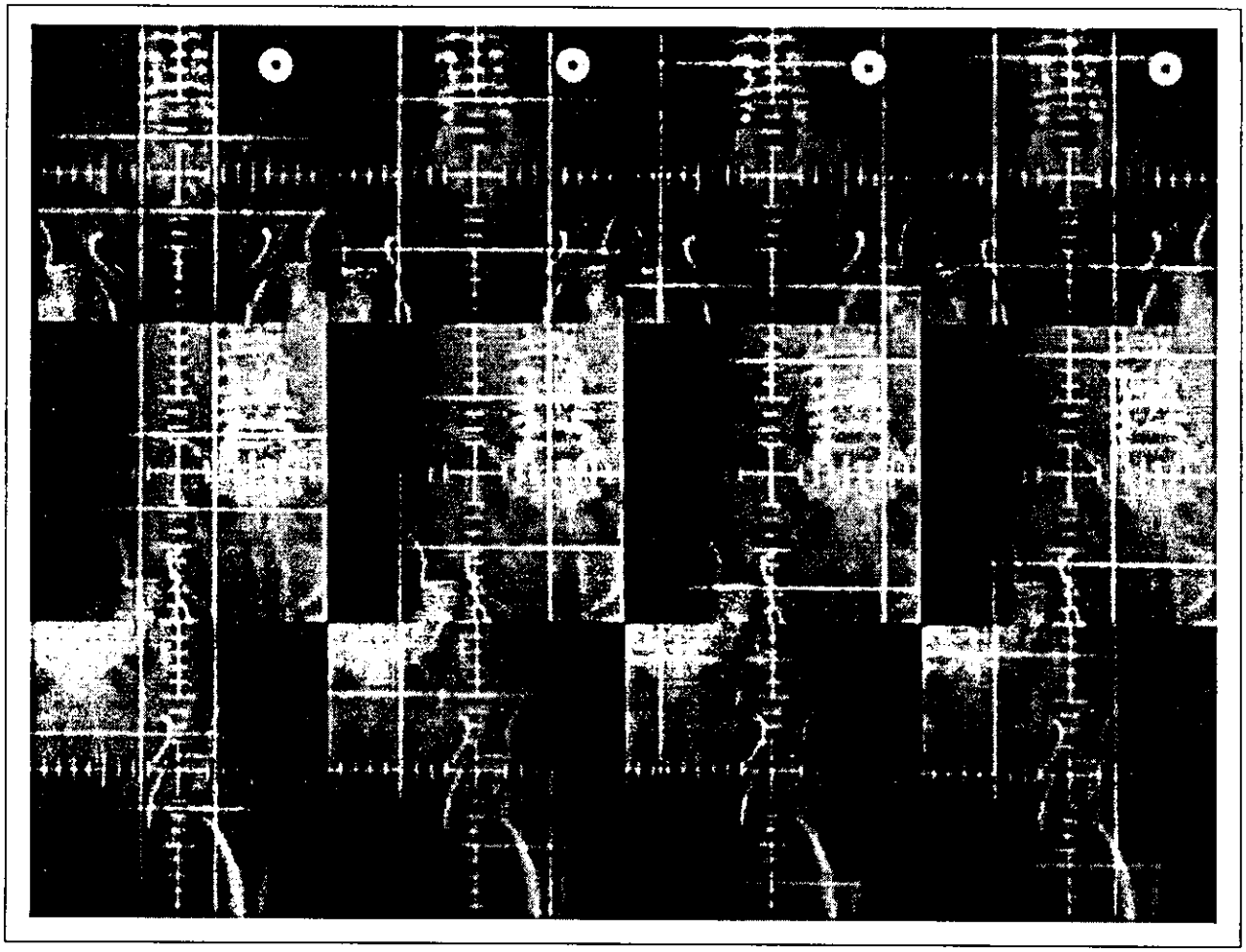

Fig. 1 All simulation images.
Top to bottom: the isocenter is located in the central part of the sacrum, the iliac bone, and the hip joint. Left to right: field shape is 5 cm sq., 10 cm sq., 15 cm sq., and 14×8 cm (asymmetrical).

イメージの間の照射野のズレを，コンピュータを用いた画像解析で定量的に検出する方法を開発し，骨盤領域の矩形照射野を対象としてその有用性を調べた．また観察者の判断を介在させずに，つまり個々の画像に応じた人為的なパラメータを入力せずに検出可能であるかを検討した．

1．使用機器および対象

1-1 使用機器

X線位置決め装置：Ximatron(Varian)
診療用高エネルギー放射線発生装置：Clinac2300C/D (Varian)
骨盤部人体ファントム：PBU-10(京都科学)
フィルムスキャナ：VXR-12 X-ray Film Scanner (Vidar)
コンピュータ：Windows2000(Microsoft)ベースのパーソナルコンピュータ
プログラム開発環境：Visual C++ Ver6.0(Microsoft)

1-2 対象

骨盤部人体ファントムを用い，シミュレーションイメージはアイソセンタ3種類(Fig. 1上段から仙骨中央部，腸骨部，股関節部)について，それぞれ照射野サイズ4種類(Fig. 1左列から5cm×5cm，10cm×10cm，15cm×15cm，頭尾方向14cm非対称×左右方向8cm非対称)を撮影した(計12枚)．

各シミュレーションイメージに対して，そのアイソセンタを既知量(A：シミュレーションイメージのアイソセンタ通り，B：シミュレーションイメージのアイソセンタより頭側へ5.0mm，C：同尾側へ10.0mm，D：同向かって左側へ5.0mm，E：同向かって右側へ10.0mm，F：同尾側へ5.0mm向かって右側へ5.0mm，G：同頭側へ10.0mm向かって左側へ10.0mm)偏移させたポータルイメージを7種類撮影した(計84枚)．

上記シミュレーションイメージとポータルイメージ計84対について，提案した手法を用いたズレの検出結果と先に示した既知のズレ量とを比較した．

2. 方 法

2-1 画像処理の概略

処理の概略をFig. 2に示す．まずX線フィルムで取得したシミュレーションイメージとポータルイメージをフィルムスキャナによりディジタル化し，両画像上で共通の基準点となる照射野の中心とその4隅の座標(Fig. 3の黒印で示した位置)を検出する．これらの基準点から両画像の拡大率とフィルム上の照射野位置の違いを算出し，一方の画像を拡大，移動(線形補間)して両画像の照射野を一致させた．また照射野サイズを入力して，画素サイズをX，Y方向について独立に求めた．次に，両画像に対してコントラスト強調処理(ヒストグラムの平坦化)を行い，撮影条件とくにX線エネルギーの違いに起因するコントラスト不良を改善した．この画像に対してスムージング処理(平滑化フィルタ)，エッジ強調処理(ラプラシアンフィルタ)，2値化処理(パーセンタイル法)を順次行い，骨陰影などの比較対照となる構造を抽出した．以上の処理で得た2枚の画像間のズレの方向および大きさを，二次元の相互相関関数を計算して求めた[5, 6]．

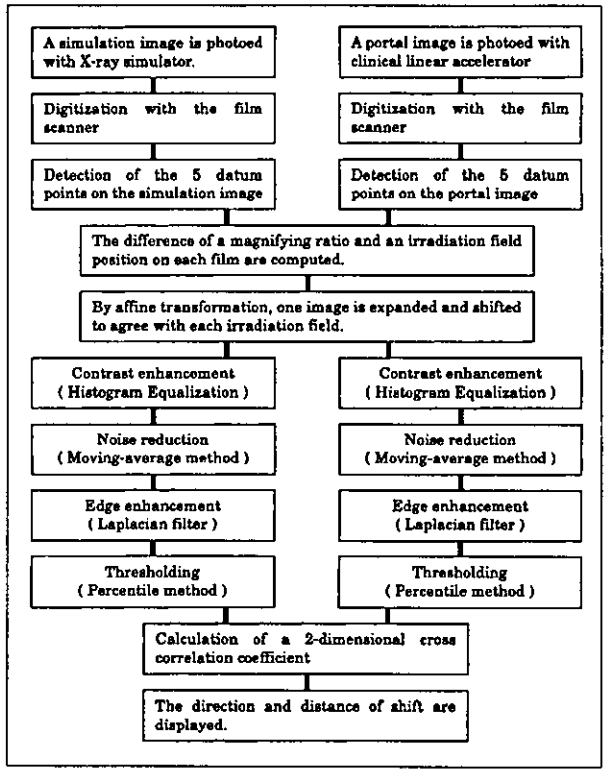

Fig. 2 Overall schema of image-processing technique.

2-2 X線フィルムのディジタル化

X線フィルムとして取得したシミュレーションイメージおよびポータルイメージをフィルムスキャナで縦(Y方向)256画素×横(X方向)256画素，グレースケール256階調でディジタル化した．その範囲は各画像の照射野辺縁から2〜8cm程度外側まで含んだ領域で，画素サイズは各画像により異なっている．

Fig. 3にシミュレーションイメージとポータルイメージの原画像の一例を示す．同じ被写体であるが撮影条件，特にX線エネルギーが違うため，両画像のコントラストは大きく異なる．

シミュレーションイメージの撮影条件は，管電圧70kVp，管電流200mA，撮影時間0.25secで，スクリーンフィルムシステムはNewA(Konica)／HS-V250(KYOKKO)を用いた．またポータルイメージの撮影条件は，X線エネルギー6MV，照射線量約3cGy(オープン)+約2cGy(照射野サイズ)で，スクリーンフィルムシステムはEC-L(Kodak)を用いた．現像条件は同じで，現像温度35°C，処理時間90sec，プロセッサは5000RA Processor(Kodak)，処理液はICM-D1／ICM-F(Kodak)を用いた．

2-3 基準点の検出

シミュレーションイメージとポータルイメージでは撮影時の幾何学的配置が異なるため，焦点ーフィルム間距離の違いが像の大きさ(拡大率)に，線束に直交する面内でのフィルムを置く位置がフィルム上での像の位置に，それぞれ影響を及ぼす．これを補正するために両画像で共通の基準点となる照射野の中心およびその4隅の座標(Fig. 3の黒印で示した位置)を検出した．処理手順を以下に示す．

(1)原画像に対して，X方向およびY方向に独立して，1ラインごとの平均画素値を計算する(Fig. 4d, 5d)．

(2)X方向およびY方向の平均画素値を1次微分する．オペレータの係数は{-1, 0, 1}を用いた．

(3)シミュレーションイメージ(Fig. 4b, c)では，微分操作でワイヤーの陰影の両側にピークが現れる．各基準点の座標はこれらの中心とした．ポータルイメージ(Fig. 5b, c)の照射野中心についても同様である．これよりX方向およびY方向それぞれ3点の座標が得られ，これらが照射野の上下縁または左右縁と中心に対応する．

以上より五つの基準点の座標が求まった．

2-4 拡大率とフィルム位置の補正

前節で求めたシミュレーションイメージとポータルイメージの基準点の座標を比較し，ポータルイメージに対するシミュレーションイメージの拡大率およびフィルム上の照射野位置の違いを算出する．X方向およびY方向の拡大率をそれぞれmag_x，mag_y，フィルム上の照射野位置の違いをそれぞれshift_x，shift_yと

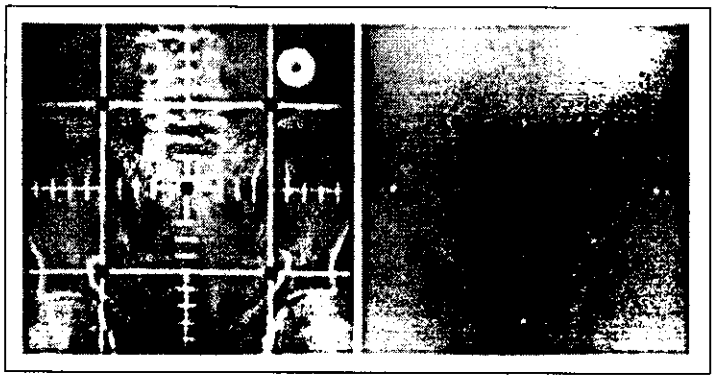

a | b

Fig. 3 Original simulation image and original portal image. The round marks in the figure show 5 datum points.
(a) Original simulation image.
(b) Original portal image.

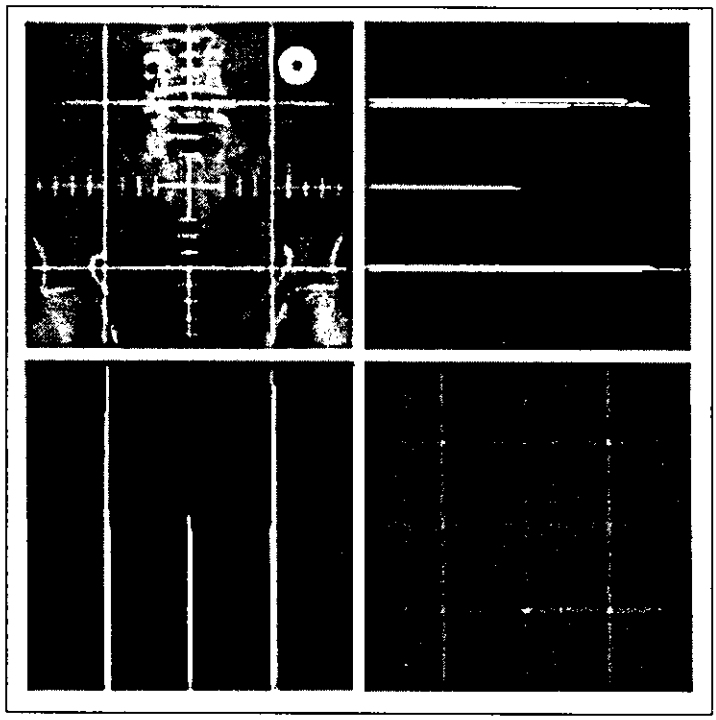

a | b
c | d

Fig. 4 Result of detection of datum points on a simulation image.
(a) Original image.
(b) Peaks detected from the profile of the Y-direction.
(c) Peaks detected from the profile of the X-direction.
(d) Profile of mean pixel values of the X and Y directions.

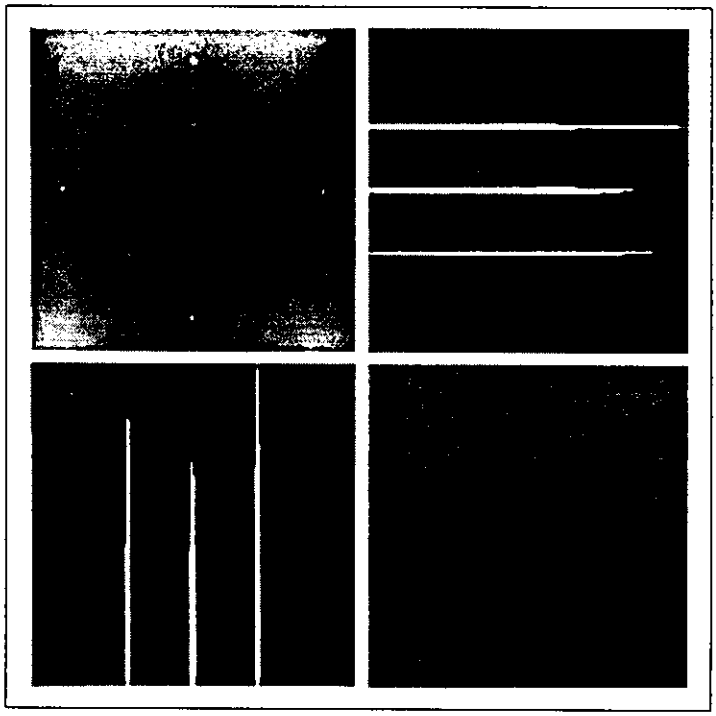

a | b
c | d

Fig. 5 Result of detection of datum points on a portal image.
(a) Original image.
(b) Peaks detected from the profile of the Y-direction.
(c) Peaks detected from the profile of the X-direction.
(d) Profile of mean pixel values of X and Y directions.